Magnetic fields in the Planck theory of sonoluminescence

Prevenslik T V
(*2E Greenery Court, Discovery Bay, Hong Kong*)

Abstract Sonoluminescence (SL) observed in the cavitation of water may be explained by the Planck theory of SL that treats the bubbles as collapsing miniature masers having optical waves standing in resonance with the dimensions of bubble cavity. Microwaves are created from the Planck energy of the standing waves provided the bubble wall may be treated as a perfect blackbody surface. In the ultraviolet, liquid H_2O is strongly absorbent and the bubble approaches a Planck blackbody enclosure. The microwaves are created at frequencies proportional to the bubble collapse velocity and are absorbed by the dipoles of the H_2O and other bubble wall molecules. Intense electric fields develop as the liquid H_2O bubble wall undergoes dielectric polarization. By this theory, free electrons are created in SL as the electric fields breakdown; the presence of free electrons is required if any magnetic field effect is to be observed in SL. Both local and global magnetic effects on SL are described. The local effect is based on the magnetic pressure due to the electrons moving as currents inside the bubble. The global effect is an accumulation of local effects at the voids throughout the liquid H_2O causing a reduction in the bulk modulus. Numerical solutions of the Rayleigh-Plesset (R-P) equation are presented that show the effect of applied magnetic field on SL to be the global effect causing a reduction in the bulk modulus. Consistent with the Planck theory of SL, the R-P simulations show the suppression of SL intensity with magnetic field to be parabolic and the SL intensity to be linear with collapse velocity.
Keywords Sonoluminescence, Maser, Magnetic fields

1 Introduction

The Planck theory of SL[1~4] finds basis in quantum mechanics and does not rely on high bubble gas temperatures generated by compression heating or shock waves to explain optical SL radiation and is applicable even if the bubble gas temperatures remain near ambient during collapse.[1] The bubbles were treated[2,3] as miniature IRasers containing electromagnetic waves at optical frequencies $f = c/\lambda$, where c is the velocity of light and λ is the wavelength. The electromagnetic waves are in standing resonance with a characteristic bubble dimension δ, i.e., $\delta = \lambda/2$. Standing wave resonance requires the SL fluid to be absorptive, e.g., for H_2O, standing waves occur in the IR and UV, but not the VIS. Here, IR is infrared , UV is ultraviolet, and VIS is visible light. However, a maser instead of an IRaser was used[4] to describe the collapsing bubble because of the connection made between SL and microwaves and is consistent with historical data[5] that shows microwaves along with optical waves are created in the collapse of a single bubble. Subsequently, the possibility of cold fusion by the microwaves created in SL was assessed.[6]

Experiments[7] to determine the effects of intense magnetic fields on SL were prompted by computer simulations[8] based on the standard model of SL that suggested bubble gas temperatures of $\sim 10^8$ K are created at the center of the bubble by spherical converging shock waves. The high temperatures have even been suggested the possibility of providing table top nuclear fusion.[9] Since a hot plasma at the core of the bubble is composed of charged particles, the spectral properties of the SL radiation observed as bremsstrahlung from the hot plasma should be affected by magnetic fields. However, a variation in the spectral properties of the SL radiation was not reported. The lack of a hot plasma signature may indicate that high temperatures are not occurring in bubble collapse, and is consistent with the high probability of an isothermal bubble collapse[10] in SL. In this paper, the Planck theory of SL briefly described at

Manuscript received date: 1997-06-1
Revised manuscript receirved date: 1998-07-14

the Symposium on SL[11] and presented at the ICA/ASA Conference [12] is assessed for consistency with the effects of magnetic fields on SL.[7]

2 Theoretical background

The Planck theory of SL requires the presence of free electrons or currents in the bubble to describe the effects of magnetic field on SL. Providing the SL fluid is polar, say H_2O, free electrons and currents[11] are created as the intense electric fields that accompany dielectric polarization breakdown. The H_2O molecule has a large dipole moment and a dielectric constant making H_2O the optimum SL fluid. But low level SL intensity may be found in SL fluids that do not have a dipole moment as in the liquid state dielectric polarization only requires a dielectric constant greater than unity. Since the free electrons may interact with an applied magnetic field, the Planck theory of SL implicitly includes a magnetic effect. However, the presence of free electrons is not limited to the bubble alone; free electrons may also be created at any collapsing void in the liquid H_2O. Voids occur because SL fluids are soluble to gases. Of particular interest are the voids that exist in the liquid H_2O adjacent to the acoustic drive transducer and are of significance if the effect of magnetic fields on SL is a reduction in the bulk modulus of H_2O. Both local and global magnetic effects are considered here. Local effects are those occurring from the free electrons within the bubble, whereas global effects are those occurring from free electrons at the voids throughout the liquid H_2O. The effect of an external magnetic field is derived for the spherical bubble shape referred to as single bubble SL, SBSL. The SBSL derivation upper bounds the magnetic pressure in a collapsing void which most likely is not spherical.

With regard to the local effect, the polarization[11] induced electrical fields lead to electron emission in the bubble wall as the polarization induced electric fields breakdown. Hence, a sheet of static charge Q_{surf} may be envisioned on the bubble wall surface comprising both free Q_{free} and bound Q_{bound} charges. In the presence of an external magnetic field **B**, electromagnetic forces $\mathbf{F}=\mathbf{K}\times\mathbf{B}$ act to set the free charge Q_{free} in motion. The bound charge Q_{bound} is not affected. The moving sheet of charge Q_{free} becomes an electrical current sheet **K** running on the bubble wall surface in the counterclockwise direction about the magnetic field lines **B** as shown in Fig.1.

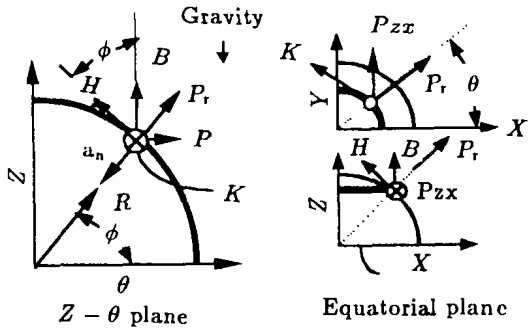

Fig.1 Spherical bubble-electromagnetic forces

The current sheet **K** at the bubble wall boundary is related to the magnetic field **H** given by the vector equation,

$$\mathbf{H} = \frac{1}{2}\mathbf{K} \times \mathbf{a}_n \tag{1}$$

where, $\mathbf{a}_n$ is the unit normal vector pointing inside the bubble. Since the current sheet **K** vector points in the counterclockwise direction around the magnetic field **B**, the magnetic field **H** vector is directed in the azimuth direction away from the equatorial plane. The **H** vector is not paralled to the **B** field, but may be resolved into a horizontal and vertical components ($\mathbf{H}_H$, $\mathbf{H}_V$). The pressure vector **P** points along the θ axis and is given by,

$$\mathbf{P} = \mathbf{K} \times \mathbf{B} = \mathbf{K} \times (\mu_0 \mathbf{H}_V) = \mathbf{K} \times (\mu_0 \mathbf{H}\cos\phi) = \mathbf{K} \times (\mu_0 \frac{1}{2}\cos\phi \cdot \mathbf{K} \times \mathbf{a}_n) \tag{2}$$

The magnitude $|\mathbf{P}|$ of the pressure **P**,

$$|\mathbf{P}| = \frac{1}{2}\mu_0 \times \cos\phi \times \mathrm{K}^2 \tag{3}$$

where, K is the current sheet in A/m. The pressure $\mathbf{P}_r$ acts in the radial R direction and has a

magnitude, $|\mathbf{P}_r| = |\mathbf{P}|\cos\phi = \frac{1}{2}\mu_0 \times \cos^2\phi\, K^2$. Now, $H = B/(\cos\phi \cdot \mu_0) = K/2$ and $K = 2B/(\cos\phi\ \mu_0)$. Hence,

$$|\mathbf{P}_r| = 2B^2/\mu_0 \tag{4}$$

The magnitude of the pressure $|\mathbf{P}_{zx}|$ acting normal to the Z-X plane is,

$$|\mathbf{P}_{zx}| = |\mathbf{P}_r|\cos\phi\sin\theta \tag{5}$$

The incremental total force $\mathrm{d}|\mathbf{F}_{zx}|$ in the Z-X plane,

$$\mathrm{d}|\mathbf{F}_{zx}| = |\mathbf{P}_{zx}|\, R\mathrm{d}\phi \cdot R \cdot \cos\phi\,\mathrm{d}\theta = |\mathbf{P}_r|\, R^2\cos^2\phi\,\mathrm{d}\phi\sin\theta\,\mathrm{d}\theta$$

$$= (2B^2R^2/\mu_0)(\cos^2\phi \cdot \mathrm{d}\phi \cdot \sin\theta\,\mathrm{d}\theta) \tag{6}$$

Integrating over the spherical bubble,

$$|\mathbf{F}_{zx}| = \frac{2B^2R^2}{\mu_0}\int_0^{\pi/2}\cos^2\phi\,\mathrm{d}\phi\int_0^{\pi/2}\sin\theta\,\mathrm{d}\theta = \pi B^2R^2/(2\mu_0) \tag{7}$$

The magnetic pressure P_{magnetic} is given by the force balance, $|\mathbf{F}_{zx}| = \pi P_{\mathrm{magnetic}}R^2/4$. Hence,

$$P_{\mathrm{magnetic}} = 2B^2/\mu_0 \tag{8}$$

3 Numerical simulations

In the Planck theory of SL, the collapse velocity V_{collapse} is derived from the Rayleigh-Plesset (**R-P**) equation[13] for a spherical bubble of radius R as a function of time t. Both local and global magnetic effects were simulated. However, the **R-P** simulations of local effects showed the negative magnetic pressure (P_{magnetic} given in Eq.(8)) was not sufficient to overcome the inertia of the collapsing bubble walls; the details of which are not presented here. Rather, the **R-P** simulation showed the effect of magnetic field in SL to be the global effect described by a lowering of the acoustic drive pressure P_a caused by a reduction in the bulk modulus K_{bulk} of the liquid H_2O. This finding suggests free electrons are created in the liquid H_2O which in the presence of a strong magnetic field B act to increase the void dimensions and the inter-molecular spacing between liquid molecules thereby lowering the bulk modulus K_{bulk}.

The **R-P** equation modified for global magnetic effects is:

$$P_{\mathrm{vapor}} + P_{\mathrm{gas}} - [(P_a - P_{\mathrm{mag}})\sin(\omega t + \phi) - P_{\mathrm{amb}}] = \rho\left[R\frac{\mathrm{d}^2R}{\mathrm{d}t^2} + \frac{3}{2}\left(\frac{\mathrm{d}R}{\mathrm{d}t}\right)^2\right] \tag{9}$$

where, P_{vapor} and P_{gas} are the pressure of the H_2O vapor and the externally supplied bubble gas (air, argon, etc.) within the bubble, P_{amb} is the ambient pressures, P_a is the acoustic drive pressure amplitude, and P_{mag} is the magnetic pressure, the pressure given in $\mathrm{N/m^2}$. Viscosity and surface tension are neglected. The magnetic pressure P_{mag} enters the **R-P** equation through a reduction in the acoustic drive pressure amplitude from P_a to (P_a-P_{mag}). P_{mag} is described later and is not the P_{magnetic} given in Eq.(8). Liquid density ρ is in $\mathrm{kg/m^3}$. The acoustic drive circular frequency ω is in rad/s ($\omega = 2\pi f$), and ϕ is a phase angle.

The effect of magnetic fields in SL as a reduction in the bulk modulus K_{bulk} may be understood by considering the acoustic drive amplitude ($P_a - P_{\mathrm{mag}}$) as the harmonic pressure generated in the liquid H_2O by the volumetric strain $\Delta V/V$ induced in the sample by the amplitude A of the acoustic transducer. Assuming a spherical sample of radius R_{sample} in the 50 mm bore of the Bitter magnet, $\Delta V/V \sim 3A/R_{\mathrm{sample}}$, where $A \sim A_0\sin(\omega t + \phi)$ is the displacement of the drive transducer, i.e., $(P_a - P_{\mathrm{mag}}) \sim 3K_{\mathrm{bulk}}A_0/R_{\mathrm{sample}}$. Hence, a first order estimate gives $K_{\mathrm{bulk}} \sim (P_a - P_{\mathrm{mag}})\, R_{\mathrm{sample}}/(3A_0)$. Because of the displacement loading in the small sample, the effect of magnetic fields in SL may be due solely to

the reduction in the bulk modulus of the liquid H_2O adjacent to the transducer surface. Since data on the effect of magnetic fields on the bulk modulus of liquid H_2O is not known, the magnetic pressure P_{mag} was deduced from the phase diagram (Fig.3 of Ref.[7]) as the line that separates the region of no SL from the region of SL. At 20°C, the data fit is $P_{mag} \sim a_0 B^2$ atm, where $a_0 \sim 0.0031\,\mathrm{atm/T^2}$. For example, at B=7 T and $P_a \sim 1.68$ atm (Fig.1 of Ref.[7]), a transducer amplitude $A_0 \sim 5\mu$m and a sample radius $R_{sample} \sim 25$ mm gives $K_{bulk} \sim 0.257 \times 10^9$ GPa. In the absence of a magnetic field, $K_{bulk} \sim 0.282 \times 10^9$ Pa. In contrast, the bulk modulus of liquid H_2O in non-SL applications (without entrained air) is about 2.2×10^9 GPa. However, experimental data on the lowering of the bulk modulus of liquid H_2O by magnetic fields during SL, say by measurements of sonic velocity, are required to confirm these predications.

In the application of the **R-P** equation, it is important to note the solutions are only valid in describing the collapse of an ideal 3-D spherical cavity in the absence of compressive instability. An ideal 3-D spherical collapse requires a very high internal bubble pressure created by the compression of externally supplied bubble gases or the H_2O vapor to maintain a stable spherical shape as the radius vanishes. Under these conditions, the collapse velocity $V_{collapse}$ is found from the **R-P** solution,

$$V_{collapse} \sim \frac{dR}{dt} \tag{10}$$

where, dR/dt is the rate of change of the bubble radius R. However, a bubble gas pressure P_{gas} increase does not occur because the gas molecules stick to the bubble wall during bubble expansion[10] and are not available to be compressed to the very high pressure necessary for a stable bubble collapse. The H_2O vapor alone is present as the bubble collapses. If the collapse is slow, say greater than about 1μs, the vapor pressure P_{vapor} remains[14] in equilibrium at the temperature of the liquid H_2O walls. For H_2O at 20°C, the vapor pressure $P_{vapor} \sim 2339$ Pa would be maintained during collapse. But at SL bubble collapse velocities $V_{collapse} \sim 100$m/s, the **R-P** simulations show the collapse time is less than about 0.5μs and the H_2O vapor may no longer be considered in equilibrium with the liquid H_2O walls. Decreased bubble volume tends to increase the H_2O vapor pressure. But the molecules of H_2O vapor during collapse (like the bubble gas molecules during expansion) that collide with and stick to the liquid bubble wall represent a mass loss of vapor and a decrease in vapor pressure within the bubble. For a sticking coefficient[15] of 0.5, the **R-P** simulations show an increase in H_2O vapor pressure due to the decreased volume that is fully compensated by the pressure decrease by mass loss. This means the **R-P** equations are only valid during bubble collapse if the pressure in the liquid surface does not exceed vapor pressure of H_2O at the temperature.

Without significant internal pressure (by the compression of the bubble gases and H_2O vapor) as the bubble collapses, the bubble wall surface is unstable and breaks-up. This suggests a bubble collapse comprising a near continuum of radially disposed micro-jets ejecting liquid H_2O clusters into the bubble interior. Under these conditions, Eqs.(9) and (10) are no longer valid. In the modified **R-P** solution, the velocity dR^*/dt at the bubble radius R^* at which instability occurs is used thereafter to compute the collapse velocity $V_{collapse}$. Applying the Bernoulli equation to an 1D streamline between R^* and the tip of the micro-jet (corresponding to the bubble surface) gives a collapse velocity $V_{collapse}$,

$$V_{collapse} \sim \sqrt{\left(\frac{dR^*}{dt}\right)^2 + \frac{2}{\rho}(P^* - P_{vapor})} \sim \frac{dR^*}{dt} \tag{11}$$

where, P^* is the pressure at R^*. Since $P^* \sim P_{vapor}$, the pressure contribution to collapse velocity $V_{collapse}$ is negligible. The modified **R-P** simulations including the 1-D Bernoulli effect after instability give collapse velocities $V_{collapse} \sim 80$ to 120 m/s at the time the bubble walls collide. Stagnation pressures in bringing the liquid H_2O bubble walls to rest are quite high and vary from 100 to 250 atm.

4 Comparisons with experimental data

In the Planck theory of SL, the SL intensity I_{SL} is proportional to the collapse velocity $V_{collapse}$ provided a threshold velocity V_{thresh} is exceeded. Hence, the SL intensity I_{SL} α

(V_{collapse}-V_{thresh}), where the threshold velocity V_{thresh} is the collapse velocity V_{collapse} at the threshold below which SL is not observed. The **R-P** equations (Eqs.(9) and (10)) modified for the 1-D Bernoulli effect after instability (Eq.(11)) are used to compute the collapse velocity V_{collapse} for a given drive amplitude (P_a-P_{mag}), where $P_{\text{mag}} \sim a_0 B^2$. Collapse velocity differences (V_{collapse}-V_{thresh}) are computed and normalized. Details are described as follows:

(a) The collapse velocity V_{collapse} for a given acoustic pressure P_a, say $P_a \sim 1.68$ atm, is computed at different B fields. The threshold magnetic B_{thresh} field is defined as the B field above which SL is not observed, i.e., B_{thresh} is the B-field at zero I_{SL} and for $P_a \sim 1.68$ atm, $B_{\text{thresh}} \sim 7$T. V_{thresh} is assigned the collapse velocity found at B_{thresh}. For $P_a \sim 1.68$ atm, Fig.2 shows the difference between collapse and threshold velocity (V_{collapse}-V_{thresh}) to be closely fit by a parabolic relation with the B field,

$$V_{\text{collapse}} - V_{\text{thresh}} = a - bB^2 \qquad (12)$$

where, a, b are constants depending on the acoustic drive amplitude P_a. In the Planck theory of SL, the SL intensity I_{SL} α (V_{collapse}-V_{thresh}). Therefore, SL intensity is also parabolic with the B field. Hence, the Planck theory of SL is consistent with the experimental data (Fig.1 of Ref.[7]) that shows the SL intensity to be parabolic with B field.

The Planck theory of SL requires I_{SL} to be linear with V_{collapse}. For a measured I_{SL}, the collapse velocity V_{collapse} may be computed with the **R-P** equation from the measured B field using the data in Fig.1 of Ref.[7]. For $P_a \sim 1.68$ atm, the measured I_{SL} is plotted against the computed V_{collapse} in Fig.3. Consistent with the Planck theory of SL, I_{SL} is observed to be linear with V_{collapse}.

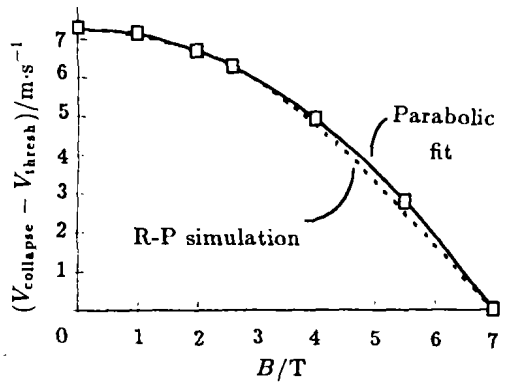

Fig.2 Collapse velocity difference vs magnetic field
Acoustic drive amplitude $P_a \sim 1.68$ atm

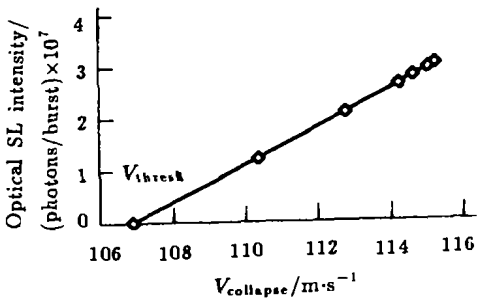

Fig.3 Optical SL intensity and collapse velocity acoustic drive amplitude $P_a \sim 1.68$ atm

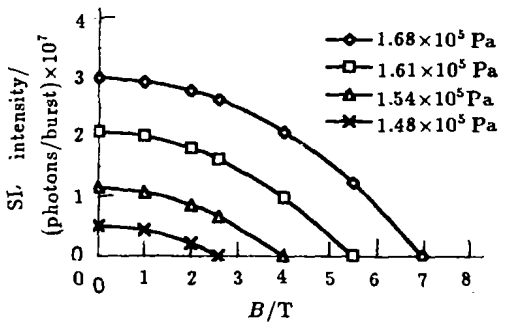

Fig.4 Suppression of optical SL intensity with magnetic field

(b) The procedure in (a) is repeated for acoustic drive amplitudes P_a (1.61, 1.54, and 1.48 atm).

(c) The collapse velocity difference (V_{collapse}-V_{thresh}) for different drive pressure P_a amplitudes at zero B field are normalized to each other by the respective range of collapse velocities. For $P_a \sim 1.68$ and 1.48 atm,

$$\frac{I_{\mathrm{SL},P_a\sim 1.68\,\mathrm{atm}}}{I_{\mathrm{SL},P_a\sim 1.48\,\mathrm{atm}}} = \frac{(V_{\mathrm{collapse},B\sim 0} - V_{\mathrm{thresh},B\sim 7\,\mathrm{T}})_{P_a\sim 1.68\,\mathrm{atm}}}{(V_{\mathrm{collapse},B\sim 0} - V_{\mathrm{thresh},B\sim 2.6\,\mathrm{T}})_{P_a\sim 1.48\,\mathrm{atm}}} \sim 6 \quad (13)$$

and explains why a 15% increase in the acoustic drive P_a pressure (from 1.48 to 1.68 atm) gives a sixfold increase in SL intensity.

(d) After a final normalization to obtain the SL intensity in units (optical photons/burst), the **R-P** results plotted in terms of the B-field suppression are shown in Fig.4. The experimental data for optical SL intensity in Fig.1 of Ref.[7] is not shown, but is almost identical to the **R-P** results.

5 Conclusions

The Planck theory of SL is consistent with the experimental data[7] on the effects of magnetic fields on SL, but data on the effects of magnetic field on the bulk modulus of liquid H_2O with entrained air at SL conditions are required for confirmation. Measurements of sonic velocity within the test cell during SL are recommended.

Provided the collapse velocity is above threshold, the SL intensity at a given magnetic field may be enhanced by decreasing the ambient temperature. A decrease in ambient temperature reduces the vapor pressure of liquid H_2O and the number of H_2O vapor molecules within the bubble. Since the H_2O vapor molecules strongly absorb the Planck energy of the UV waves standing in resonance with the bubble walls, the SL intensity from the bubble wall surface molecules increases as the ambient temperature is lowered. This is evident from a comparison of SL intensity at 10 and 20°C (Fig.2 of Ref.[7]) and may further be enhanced by a lowering of ambient temperature near the freezing point. Similarly, an increase in the acoustic pressure amplitude (Fig.1 of Ref.[7]) increases the collapse velocity and thereby increases the SL intensity.

Acknowledgements

The advice by Li Yi-Wei of the Taiyuan Heavy Machinery Institute, PRC are acknowledged.

References

1 Prevenslik T V. Biological effects of ultrasonic cavitation. Fifth International Conference on Cold Fusion, April 9-13, 1995. Monte Carlo, Monaco
2 Prevenslik T V. Sonoluminescence: IRaser?. Ninth International Conference on Photoacoustic and Photothermal Phenomena. June 27-30, 1996, Nanjing University, Nanjing, China
3 Prevenslik T V. Sonoluminescence in the Planck theory. Submitted to Chin J Acoustics, 1997
4 Wang C H, Zhang D Z. Chin J Acoustics (in Chinese), 1964, 1(2):59
5 Prevenslik T V, Wu Z, Chen F. Sonoluminescence: Femtosecond lasing in the microwave region. International Conference on Laser Physics and Quantum Optics. Hong Kong, January 7-9, 1997. Singapore: Springer-Verlag. 1997.84
6 Prevenslik T V. Nuclear Science and Techniques, 1997, 8(2):94
7 Young J B, Schmiedel T, Kang W. Phys Rev Lett, 1996, 77:4816
8 Wu C C, Roberts P H. Phys Rev Lett, 1993, 70:3424
9 Moss W C, Clarke D B, White J W *et al.* Phys Lett A, 1996, 211:69
10 Prevenslik T V. Nucl Sci Tech, 1997, 8(4):236
11 Prevenslik T V. Sonoluminescence: The effect of magnetic field in the Planck theory. Symposium on Sonoluminescence, University of Chicago, Sep 12-13, 1997
12 Prevenslik T V. Sonoluminescence: The effect of magnetic fields in the Planck Theory. 16th International Conference on Acoustics, Seattle, June 20-26, 1998
13 Brennen C E. Cavitation and bubble dynamics. New York: Oxford University Press, 1995
14 Hammitt F G. Cavitation and multiphase flow phenomena. New York: McGraw-Hill, 1980
15 Valuev A A, Zheludkov S V, Iskakov A N *et al.* Russ J Phys Chem, 1992,66(2):137